

## Thermal stability of epitaxial SrRuO<sub>3</sub> films as a function of oxygen pressure

Ho Nyung Lee,<sup>a)</sup> Hans M. Christen, Matthew F. Chisholm, Christopher M. Rouleau, and Douglas H. Lowndes

Condensed Matter Sciences Division, Oak Ridge National Laboratory, Oak Ridge, Tennessee 37831

(Received 26 January 2004; accepted 19 March 2004; published online 5 May 2004)

The thermal stability of electrically conducting SrRuO<sub>3</sub> thin films grown by pulsed-laser deposition on (001) SrTiO<sub>3</sub> substrates has been investigated by atomic force microscopy and reflection high-energy electron diffraction (RHEED) under reducing conditions (25–800 °C in 10<sup>-7</sup>–10<sup>-2</sup> Torr O<sub>2</sub>). The as-grown SrRuO<sub>3</sub> epitaxial films exhibit atomically flat surfaces with single unit-cell steps, even after exposure to air at room temperature. The films remain stable at temperatures as high as 720 °C in moderate oxygen ambients (>1 mTorr), but higher temperature anneals at lower pressures result in the formation of islands and pits due to the decomposition of SrRuO<sub>3</sub>. Using *in situ* RHEED, a temperature and oxygen pressure stability map was determined, consistent with a thermally activated decomposition process having an activation energy of 88 kJ/mol. The results can be used to determine the proper conditions for growth of additional epitaxial oxide layers on high quality electrically conducting SrRuO<sub>3</sub>. © 2004 American Institute of Physics.  
[DOI: 10.1063/1.1753650]

Advances in epitaxial thin film growth techniques have enabled the growth of high quality insulating crystalline oxides, such as SrTiO<sub>3</sub> (cubic with  $a=0.391$  nm), on Si substrates (cubic with  $a=0.543$  nm).<sup>1,2</sup> However, there still remains an equally high demand for an epitaxial electrically conducting oxide to replace conventional choices, such as poly-Si, for gate electrodes. Among the conducting perovskites, for example, SrRuO<sub>3</sub> [pseudocubic with  $a=0.393$  nm (calculated from the orthorhombic lattice parameters of  $a=0.557$ ,  $b=0.553$ , and  $c=0.785$  nm)<sup>3</sup>] is very promising,<sup>4–6</sup> since it is well lattice matched to other perovskite-type oxides, and if grown with sufficiently high quality, may permit full *monolithic* integration of crystalline oxides into complex Si-based devices. In order to employ SrRuO<sub>3</sub> in this environment, however, it must remain stable under the reducing (low oxygen pressure) conditions typical of molecular beam epitaxy (MBE) or pulsed laser deposition (PLD). However, there are few reports on the degradation mechanism of ferroelectric capacitors with polycrystalline SrRuO<sub>3</sub> bottom and/or top electrodes by annealing in hydrogen or forming gas.<sup>7–10</sup> Moreover, there have been no systematic studies on the stability of SrRuO<sub>3</sub> itself, especially under those conditions at which most high quality crystalline oxide films are grown by MBE and PLD.

Here we report on the thermal stability of high quality SrRuO<sub>3</sub> thin films that have atomically flat surfaces exhibiting only single unit-cell terrace steps (“single-stepped”), under various oxygen pressures and temperatures.

Prior to film growth, single-stepped SrTiO<sub>3</sub> substrates<sup>11,12</sup> were prepared by dipping as-received SrTiO<sub>3</sub> wafers (miscut tolerance <0.1°) first in water for a few seconds and then in commercially available, buffered oxide etch (BOE) ( $pH\approx 4.5$ , BOE:H<sub>2</sub>O=1:10) for 30 s, followed by

thermal annealing at 1100–1200 °C for 1 h depending on the miscut angle of the substrates. (Substrates with a lower miscut angle require a higher annealing temperature in order to form straight terrace edges.) SrRuO<sub>3</sub> films were then grown by PLD using a KrF excimer laser ( $\lambda=248$  nm) at a substrate temperature of 700 °C in 100 mTorr O<sub>2</sub>. For the reflection high-energy electron diffraction (RHEED) investigation, the samples were transferred in air to a different chamber equipped with RHEED and a residual gas analyzer (RGA). For these experiments, the samples were remounted onto a heater plate with Ag paint, cured in air at ~200 °C for 5 min, and then loaded into the chamber, which was pumped to below  $1\times 10^{-7}$  Torr. For RHEED investigations at moderately high oxygen pressures (up to 10 mTorr for this study), differential pumping allowed us to keep the pressure within the filament region of the e-gun below  $5\times 10^{-6}$  Torr, but electron scattering resulted in weakened patterns at the highest pressures. The RHEED patterns were recorded during heating of the samples at a constant ramp rate of 15 °C/min up to 800 °C at various fixed pressures. The surface topography of the SrRuO<sub>3</sub> films was then investigated in air by *ex situ* atomic force microscopy (AFM) working in tapping mode, in order to compare the surfaces before and after the RHEED experiments. The film–substrate interface and the upper surface of as-grown films were investigated by Z-contrast scanning transmission electron microscopy (Z-STEM) of cross-sectional samples in which a SrRuO<sub>3</sub> layer was sandwiched between the SrTiO<sub>3</sub> substrate and a subsequently grown SrTiO<sub>3</sub> film.

Figure 1(a) shows an AFM topographic image of an as-grown SrRuO<sub>3</sub> film. There were no features on the surface except for the terrace edges which mimicked those of the SrTiO<sub>3</sub> substrate [Fig. 1(b)]. The terrace height (~0.4 nm) corresponds to a single unit cell of SrRuO<sub>3</sub> (0.393 nm). Since it is known that SrRuO<sub>3</sub> nucleates in a layer-by-layer mode but then grows via a step-flow mechanism,<sup>13</sup> growing

<sup>a)</sup>Electronic mail: hnlee@ornl.gov

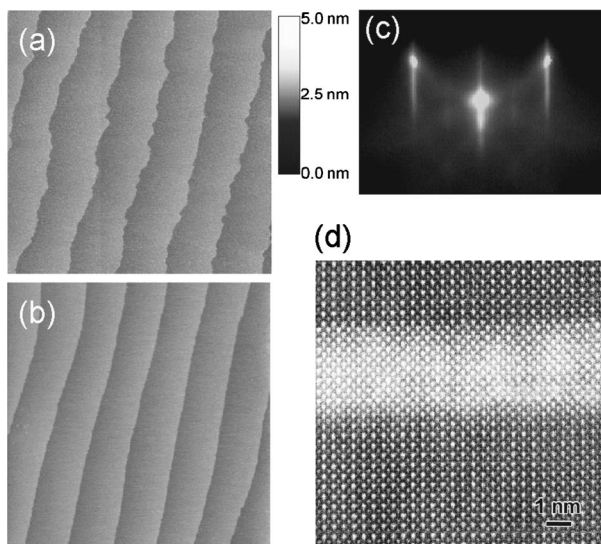


FIG. 1. AFM topographic images of (a) an as-grown SrRuO<sub>3</sub> film and (b) of a (001) SrTiO<sub>3</sub> substrate (image size: 3×3 μm<sup>2</sup>); (c) RHEED pattern along the <100> direction of the as-grown SrRuO<sub>3</sub> taken at 25 °C in vacuum (~1×10<sup>-7</sup> Torr); (d) atomically abrupt interfaces are observed in the cross-sectional Z-STEM image of a SrTiO<sub>3</sub>/SrRuO<sub>3</sub> (~3.6 nm) bilayer on SrTiO<sub>3</sub>.

films with atomically flat surfaces is possible even without having to carefully determine the termination point of the growth. As seen in the *ex situ* RHEED pattern in Fig. 1(c), for example, a bright specular spot and diffraction spots with a well developed pattern of Kikuchi lines, as well as the secondary Laue pattern (not shown), are usually observed from SrRuO<sub>3</sub> thin films even after exposure to air, confirming again the very flat, near-perfect, and stable surface of our starting material. A cross-section Z-STEM image [Fig. 1(d)] not only further confirms the quality of these layers, since atomically abrupt interfaces are observed at both the substrate and overlayer, but also demonstrates the value of these films as buffer layers. Note that the interface with the substrate is compositionally broader than that with the subsequently grown SrTiO<sub>3</sub> film; the reason for this has not been determined.

Figure 2 shows *in situ* RHEED patterns at temperatures up to 720 °C at various oxygen pressures, corresponding to the range of parameters under which many epitaxial oxides are typically grown. Also shown are the *ex situ* AFM images obtained on the samples after this thermal treatment. In the extreme case of a SrRuO<sub>3</sub> film heated in vacuum (~1×10<sup>-6</sup> Torr at 720 °C), a drastic deterioration of the surface quality was observed at a relatively low temperature (450–500 °C), as evidenced by RHEED patterns showing signs of electron transmission through small islands. (Only an insignificant change was noted upon further heating to 800 °C.) Correspondingly, an AFM image of a sample after heating to 560 °C [Fig. 2(a)] exhibited a roughened surface. In striking contrast, even a very small amount of oxygen can improve the surface stability. Under these conditions, different types of defects appear on the surface as a function of oxygen pressure, including tiny islands [Fig. 2(b)] and pits [Fig. 2(c)]. To completely stabilize the surface at 720 °C and preserve the single-stepped terraces, at least 1 mTorr of oxygen is required.

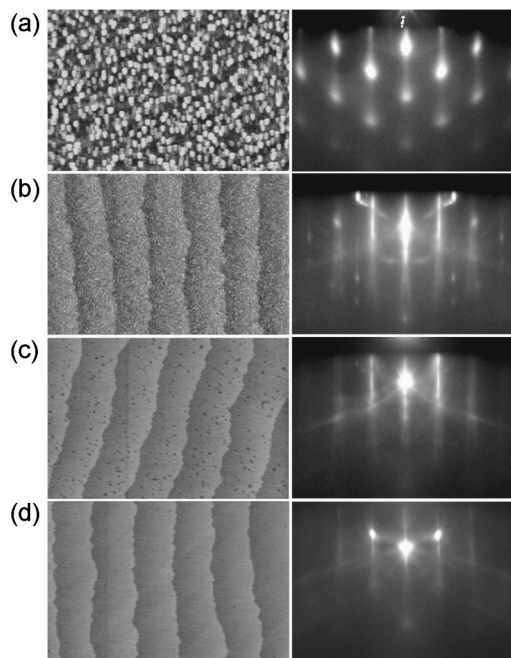


FIG. 2. *Ex situ* AFM topographic images (left-hand side, image size: 3×2 μm<sup>2</sup>) and corresponding *in situ* RHEED patterns along the <100> direction (right-hand side) of SrRuO<sub>3</sub> films heated up to (a) 560 °C in vacuum and to 720 °C in (b) 1×10<sup>-5</sup>; (c) 5×10<sup>-4</sup>; and (d) 1×10<sup>-3</sup> Torr O<sub>2</sub>. The rms roughness values on a terrace of the AFM images are (a) 1.578, (b) 0.162, (c) 0.125, and (d) 0.06 nm. The latter value is identical (within experimental error) to that of a SrTiO<sub>3</sub> substrate. The height scale of the AFM images ranges from 0 to 15 nm (a) or to 5 nm [(b)–(d)].

The thermal stability of SrRuO<sub>3</sub> in the presence of oxygen is very similar to what has been reported for annealing in forming gas (3% H<sub>2</sub>+97% N<sub>2</sub>).<sup>8</sup> In those cases, adding 0.5% of oxygen to the forming gas can prevent the decomposition of SrRuO<sub>3</sub> that would normally occur when exposed to pure forming gas at 400 °C for 1 h. Halley *et al.* also reported that while the addition of 1%–2% O<sub>2</sub> to forming gas prevented decomposition even at temperatures as high as 700 °C, heating in vacuum (10<sup>-4</sup> Torr) caused the decomposition of SrRuO<sub>3</sub> to occur around 600 °C.<sup>10</sup> It is interesting to note that RuO<sub>2</sub> readily decomposes (yielding Ru and O<sub>2</sub>) in both vacuum and an inert gas ambient,<sup>14</sup> and that thermodynamic investigations confirmed a possible coexistence of metallic Ru with the similar ternary ruthenate CaRuO<sub>3</sub> at low oxygen pressure.<sup>15</sup> Consequently, it is plausible to suggest that the islands seen, e.g., in Fig. 2(a), can be attributed, for example, to the formation of metallic Ru resulting in both Ru and nonstoichiometric Sr–Ru–O on the surface, as a consequence of the unstable nature of RuO<sub>2</sub>. In fact, the discontinuous RHEED spots originating from the islands [Fig. 2(a)] exhibit a slightly different horizontal spacing than the SrRuO<sub>3</sub> streaks [Figs. 2(c) and 2(d)]. However, by introducing oxygen (e.g., 10<sup>-2</sup> Torr O<sub>2</sub> at 720 °C) into the chamber, the RHEED pattern (streaky nature and spacing) partially reverts to the one observed originally. (Note that Ru oxidizes readily at 7.5×10<sup>-4</sup> Torr of oxygen at 600 K.<sup>16</sup>)

According to this RHEED investigation, samples heated in 1×10<sup>-3</sup> Torr O<sub>2</sub> remained stable up to 720 °C. However, upon further heating to 800 °C, *ex situ* AFM investigations show that one unit-cell deep pits are formed [Fig. 3(c)]. This partial decomposition of the SrRuO<sub>3</sub> surface coincides with

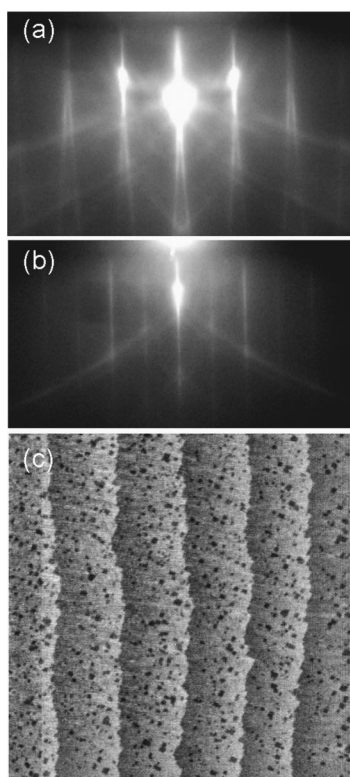


FIG. 3. RHEED patterns along (a) the  $\langle 100 \rangle$  direction and (b) the  $\langle 110 \rangle$  direction of a  $\text{SrRuO}_3$  film at  $800^\circ\text{C}$  in  $1 \times 10^{-3}$  Torr  $\text{O}_2$ , showing two streaks of the specular and diffraction spots along the  $\langle 100 \rangle$  direction, but not along the  $\langle 110 \rangle$  direction; (c) *ex situ* AFM topographic image (image size:  $3 \times 3 \mu\text{m}^2$ ) of the same sample showing single-unit cell deep pits on the surface.

the irreversible appearance of additional RHEED features: The specular spot shows a distinct splitting along the  $\langle 100 \rangle$  direction [Fig. 3(a)], while no splitting is observed along the  $\langle 110 \rangle$  direction [Fig. 3(b)]. This strong anisotropy is consistent with an interpretation of mosaic formation, similar to what is observed in  $\text{MgO}/\text{Ag}(100)$ ,<sup>17</sup> although the observation could be attributed to any superstructure or to ordered defects on the surface. Finally, we note that the same type of island formation and RHEED-line splitting at  $800^\circ\text{C}$  is still observed when the pressure is reduced by an order of magnitude, i.e., at  $1 \times 10^{-4}$  Torr (data not shown).

As a result of recording temperature-dependent RHEED observations of the  $\text{SrRuO}_3$  surface during heating at various oxygen pressures, the thermal stability for  $\text{SrRuO}_3$  has been mapped as a function of pressure and temperature, in the Arrhenius plot shown in Fig. 4. The data points of this stability diagram represent the temperatures at which the RHEED pattern changes from the normal state [i.e., as shown in Fig. 1(c)], to other patterns (including islands, pits, mosaics, superstructures, etc.). The data are consistent with a thermally activated decomposition process, having an activation energy of 88 kJ/mol. Most significantly, the diagram can be used to determine the proper conditions under which additional epitaxial oxide layers can be grown on high quality electrically conducting  $\text{SrRuO}_3$ .

In conclusion, highly particle-free, single-stepped epitaxial  $\text{SrRuO}_3$  films have been grown by PLD; AFM, Z-STEM, and RHEED investigations demonstrate a near-perfect surface quality. Thus, these layers are applicable to

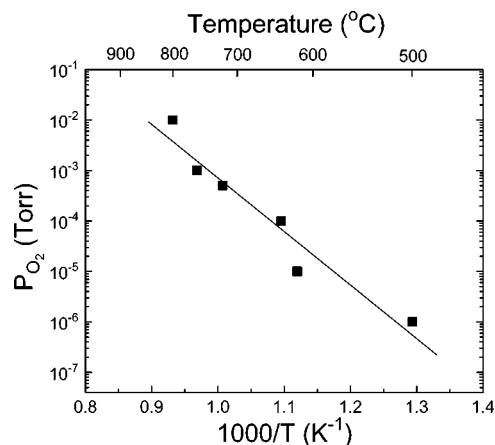


FIG. 4. Arrhenius plot of pressure vs substrate temperature of  $\text{SrRuO}_3$  epitaxial films. The data points are taken as the temperature at which the original RHEED pattern changes its appearance. The solid line corresponds to a thermally activated process with an activation energy of 88 kJ/mol.

the heteroepitaxial growth of further oxide layers in applications requiring a conducting bottom layer. Our work shows that  $\text{SrRuO}_3$  is unstable at low oxygen pressure, likely yielding metallic Ru and nonstoichiometric Sr–Ru–O at the surface, and thus requires an adequate amount of oxygen to remain stable. A temperature and oxygen pressure stability diagram delineates the required parameters for the growth of subsequent films on  $\text{SrRuO}_3$ .

This research was sponsored by the U.S. Department of Energy under Contract No. DE-AC05-00OR22725 with the Oak Ridge National Laboratory, managed by UT-Battelle, LLC, as part of a BES NSET initiative on Nanoscale Cooperative Phenomena and of the LDRD Program.

- R. A. McKee, F. J. Walker, and M. F. Chisholm, *Phys. Rev. Lett.* **81**, 3014 (1998).
- K. Eisenbeiser, J. M. Finder, Z. Yu, J. Ramdani, J. A. Curless, J. A. Hallmark, R. Droopad, W. J. Ooms, L. Salem, S. Bradshaw, and C. D. Overgaard, *Appl. Phys. Lett.* **76**, 1324 (2000).
- J. J. Randall and R. Ward, *J. Am. Chem. Soc.* **81**, 2629 (1959).
- C. B. Eom, R. J. Cava, R. M. Fleming, J. M. Phillips, R. B. van Dover, J. H. Marshall, J. W. P. Hsu, J. J. Krajewski, and W. F. Peck, Jr., *Science* **258**, 1766 (1992).
- Q. X. Jia, X. D. Wu, S. R. Foltyn, and P. Tiwari, *Appl. Phys. Lett.* **66**, 2197 (1995).
- H. N. Lee, D. Hesse, N. Zakharov, and U. Gösele, *Science* **296**, 2006 (2002).
- J.-P. Han and T. P. Ma, *Appl. Phys. Lett.* **71**, 1267 (1997).
- J. Lin, K. Natori, Y. Fukuzumi, M. Izuka, K. Tsunoda, K. Eguchi, K. Hieda, and D. Matsunaga, *Appl. Phys. Lett.* **76**, 2430 (2000).
- Y. B. Kim, J. H. Park, D. H. Hong, D. K. Choi, C. Y. Yoo, and H. Horii, *J. Appl. Phys.* **93**, 9212 (2003).
- D. Halley, C. Rossel, D. Widmer, H. Wolf, and S. Gariglio, *Mater. Sci. Eng., B* (to be published).
- M. Kawasaki, K. Takahashi, T. Maeda, R. Tsuchiya, M. Shinohara, O. Ishiyama, T. Yonezawa, M. Yoshimoto, and H. Koinuma, *Science* **266**, 1540 (1994).
- G. Koster, B. L. Kropman, G. J. H. M. Rijnders, D. H. A. Blank, and H. Rogalla, *Appl. Phys. Lett.* **73**, 2920 (1998).
- J. Choi, C. B. Eom, G. Rijnders, H. Rogalla, and D. H. A. Blank, *Appl. Phys. Lett.* **79**, 1447 (2001).
- J. A. Rard, *Chem. Rev. (Washington, D.C.)* **85**, 1 (1985).
- K. T. Jacob, K. T. Lwin, and Y. Waseda, *J. Electrochem. Soc.* **150**, E227 (2003).
- A. Böttcher and H. Niehus, *Phys. Rev. B* **60**, 14396 (1999).
- J. Wollschläger, D. Eröds, and K.-M. Schröder, *Surf. Sci.* **402–404**, 272 (1998).